九州大学大学院総合理工学府報告
第 43 巻 第 2 号 1-10 頁 令和 4 年 2 月

Engineering Sciences Reports, Kyushu University
Vol. 43, No. 2, pp. 1-10, FEB, 2022

Formation of Excited CH($A^2\Delta$, $B^2\Sigma^-$, and $C^2\Sigma^+$) Radicals by Collisions of Metastable Ne($^3P_{0,2}$) Atoms with Simple C_1~C_3 Aliphatic Hydrocarbons in a Flowing Afterglow

Masaharu TSUJI*1,2† Takahiro KOMATSU*3 Keiko UTO*1
Jun-Ichiro HAYASHI*1,2 and Takeshi TSUJI*4
†E-mail of corresponding author: tsuji@cm.kyushu-u.ac.jp

(Received November 9, 2021, accepted November 24, 2021)

CH($A^2\Delta$–$X^2\Pi_r$ $B^2\Sigma^-$–$X^2\Pi_r$, and $C^2\Sigma^+$–$X^2\Pi_r$) emission systems have been observed by dissociative excitation of such simple C_1~C_3 aliphatic hydrocarbons as CH_4, C_2H_6, C_2H_4, and C_3H_4 by collisions with metastable Ne($^3P_2$:16.62 and $^3P_0$:16.72 eV) atoms in the flowing afterglow. The emission rate constants of CH(A,B,C) from CH_4, C_2H_6, C_2H_4, and C_3H_4 were determined to be 0.082, 0.039, 0.38, and 0.59 × 10^{-13} cm^3 $molecule^{-1}$ s^{-1}, respectively. The CH(A) state was the major CH* product in all reactions, which occupied 64–92% of CH(A,B,C) products. The nascent vibrational and rotational distributions of CH(A:v'=0–2 and B:v'=0) were determined. The rotational distributions of CH(A:v'=0–2 and B:v'=0) states were expressed by single Boltzmann temperatures of 1700–4600 K and 2500–5500 K, respectively. The CH(A:v'=0 and B:v'=0) states from C_3H_4 were more rotationally excited than those from the other aliphatic hydrocarbons.

Key words: *Dissociative excitation, Aliphatic hydrocarbons, Metastable Ne* atoms, Flowing afterglow, Energy transfer, Rovibrational distribution, Superexcited state, Rydberg state*

1. Introduction

Reactions of rare gas metastable atoms with aliphatic hydrocarbons in discharge plasma are important for understanding dissociation and ionization mechanisms of mixtures of rare gas atoms and aliphatic hydrocarbons used for the fabrication of various carbon films.[1-3] Compared with extensive studies on reactions of He(2^3S:19.82 eV) and Ar($^3P_2$:11.55 eV, $^3P_0$:11.72 eV) with simple aliphatic hydrocarbons,[4-9] little work has been carried out on reactions of Ne($^3P_{0,2}$) with them because of high cost of Ne gas. We have previously studied reactions of Ne($^3P_{0,2}$) with CH_4 and C_2H_2 in a Ne flowing afterglow (FA) by observing optical emission spectra from such excited fragments as CH* and C_2* in the ultraviolet (UV) and visible region.[10,11] Rovibrational distributions of CH(A,B) were determined for the Ne($^3P_{0,2}$)/CH_4 reaction by a spectral simulation. Not only rovibrational distributions of CH(A,B) and C_2(d,C,e,D) but also emission rate constants of CH(A,B,C) and C_2(d,C,e,D) were determined for the Ne($^3P_{0,2}$)/C_2H_2 reactions. It was concluded that rotationally excited CH* and vibrationally and rotationally excited C_2* are formed via *trans*-bent Rydberg (superexcited) C_2H_2** states with elongated C≡C bond and bending mode excitation.

In order to obtain more information on reaction dynamics of acetylene, isotope effects between C_2H_2 and C_2D_2 were examined.[11] Although the reduction of emission rate constant of C_2* from C_2D_2 was consistent with a simple dissociation model from the RRKM theory, the increase in the emission rate constant of CD* did not agree with it. The *inverse* isotope effect for CD* was explained by the fact that the formation of C_2* and CH* or CD* occurs competitively, so that faster dissociation of C–H bonds suppresses the formation of CH*.

In the present study, emission spectra resulting from energy-transfer reactions of

*1 Institute for Materials Chemistry and Engineering, and Research and Education Center of Green Technology
*2 Department of Applied Science for Electronics and Materials
*3 Department of Applied Science for Electronics and Materials, Graduate Student
*4 Department of Materials Science, Shimane University

Ne($^3P_{0,2}$) atoms with CH_4, C_2H_6, C_2H_4, and C_3H_4 (allene) are measured in the Ne FA. The emission rate constants of CH(A,B,C) and rovibrational distributions of CH(A,B) are determined. On the basis of these data, energy-transfer mechanisms are discussed.

2. Experimental

The FA apparatus equipped with an optical emission detection system was the same as those reported previously.[10,11,13] The following gases were used in this study: Ne (Nippon Sanso: purity 99.55%), CH_4 (Eto Sanso: 99.0%), C_2H_6 (Eto Sanso: 99.0%), C_2H_4 (Eto Sanso: 99.0%), C_2H_6 (Eto Sanso: 99.0%), C_3H_4 (Nippon Sanso: 99.3%), and SF_6 (Seitetsu Kagaku: 99.7%).

In brief, the metastable Ne($^3P_{0,2}$) atoms were generated by a microwave discharge of high purity Ne gas operated at Ne pressures of 0.1–0.15 Torr (1 Torr = 133.3 Pa). The effect of ionic active species was examined by using an ion-collector grid placed between the discharge section and the reaction zone. A small amount of aliphatic hydrocarbons (CH_4, C_2H_6, C_2H_4, and C_3H_4) was injected into the Ne afterglow from a nozzle placed 10 cm downstream from the center of the discharge. The partial pressure of reagent gas in the reaction zone was 1–6 mTorr.

Emission spectra were observed through a quartz window placed around a reagent gas inlet. A Spex 1.25 m monochromator equipped with a Hamamatsu Photonics R376 photomultiplier was used for spectral measurements in the 300–700 nm region. The relative sensitivity of the optical detection system was calibrated using standard D_2 and halogen lamps.

3. Results and Discussion

3.1 Emission spectra and dissociative excitation processes

Figures 1a–1d show typical emission spectra obtained from the Ne afterglow reaction of CH_4, C_2H_6, C_2H_4, and C_3H_4, respectively. The CH($A^2\Delta$–$X^2\Pi_r$, $B^2\Sigma^-$–$X^2\Pi_r$, and $C^2\Sigma^+$–$X^2\Pi_r$) emission systems are identified in the 300–450 nm region. In the 305–320 nm region, a broad OH($A^2\Sigma^+$–$X^2\Pi_i$) emission system[14] resulting from dissociative excitation of impurity H_2O is overlapped with the CH(C–X) emission with a sharp peak at 314 nm. When the contribution of ionic active species to the observed emissions was examined by using the ion-collector grid,

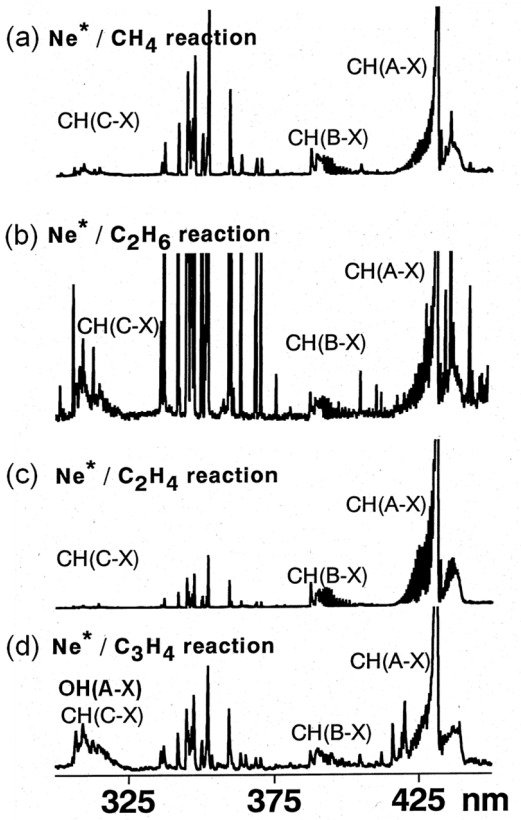

Fig. 1. Emission spectra obtained from Ne afterglow reactions of (a) CH_4, (b) C_2H_6, (c) C_2H_4, and (d) C_3H_4 (allene).

no appreciable changes were observed in the intensities of CH(A–X, B–X, and C–X). These results indicate that Ne^+ and Ne_2^+ ions do not participate in the formation of CH(A,B,C). Based on above findings, Ne($^3P_{0,2}$) atoms are responsible for the production of these emitting excited states.

Figures 2–5 show energy-level diagrams of ionization states and CH(A,B,C) states produced from CH_4, C_2H_6, C_2H_4, and C_3H_4, respectively, where ionization potentials (IPs) and dissociation limits (DLs) for the formation of each state are shown. Thermochemical and spectroscopic data reported in Refs. 15–17 are used for the calculations. The lowest IPs of CH_4, C_2H_6, C_2H_4, and C_3H_4 are 10.1–12.0 eV. Since these values are lower than the energies of Ne($^3P_{0,2}$:16.62 and 16.72 eV), M^+ (M = CH_4, C_2H_6, C_2H_4, and C_3H_4) ions can be formed by Penning ionization (1).

$$Ne(^3P_{0,2}) + M \rightarrow M^+ + Ne + e^- \quad (1)$$
(M = CH_4, C_2H_6, C_2H_4, and C_3H_4)

In the cases of C_2H_6, C_2H_4, and C_3H_4, not only the ground ionic state but also excited ionic

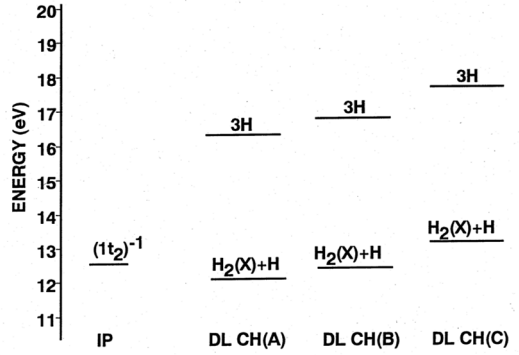

Fig. 2. Energy-level diagrams for the formation of CH(A,B,C) states from CH_4. IP and DL mean ionization potential and dissociation limit, respectively.

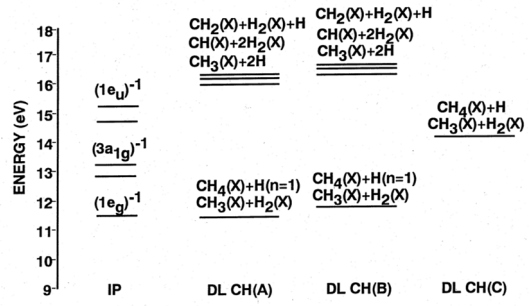

Fig. 3. Energy-level diagrams for the formation of CH(A,B,C) states from C_2H_6.

states can be formed energetically. The DLs of CH(A,B) from CH_4 and C_2H_4, and CH(A) from C_2H_6 are lower than first IPs of M. Therefore, formation of CH(A,B) via two-body electron-ion recombination processes are energetically possible.

$$M^+ + e^- \rightarrow CH(A,B) + \text{neutral products} \quad (2)$$
$$(M = CH_4, C_2H_6, C_2H_4)$$

To examine the contribution of above processes, effects of the addition of a typical electron scavenger, SF_6, was examined. SF_6 scavenges thermal electrons very rapidly:

$$e^- + SF_6 \rightarrow SF_6^- \quad (3)$$
$$k_3 = 2.2 \times 10^{-7}\ cm^3\ s^{-1}\ \text{(Ref. 18)}.$$

Little intensity changes are observed before and after SF_6 addition. Based on this result, we conclude that two-body electron-ion recombination processes (2) do not participate in the formation of CH(A,B) from CH_4, C_2H_6, and C_2H_4. Thus, two-body energy-transfer reactions between $Ne(^3P_{0,2})$ and M are responsible for the formation of CH(A,B).

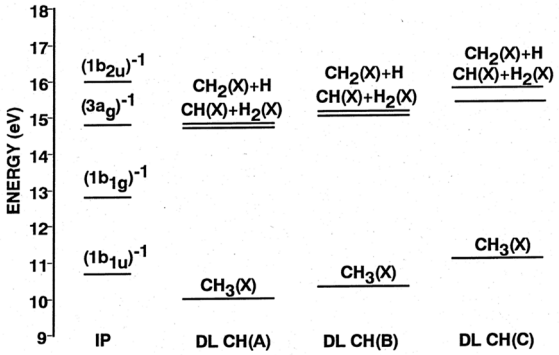

Fig. 4. Energy-level diagrams for the formation of CH(A,B,C) states from C_2H_4.

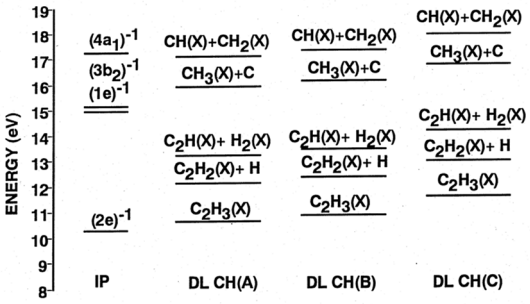

Fig. 5. Energy-level diagrams for the formation of CH(A,B,C) states from C_3H_4 (allene).

3.2 Emission rate constants of CH(A,B,C) in the $Ne(^3P_{0,2})/M$ (M = CH_4, C_2H_6, C_2H_4, and C_3H_4) reactions

Energetically possible excitation processes of CH(A,B,C) by the $Ne(^3P_2)/M$ (M = CH_4, C_2H_6, C_2H_4, and C_3H_4) atoms are as follows:

$Ne(^3P_2) + CH_4$
$\rightarrow CH(A) + H_2 + H + Ne + 4.55\ eV,$ (4a)
$\rightarrow CH(B) + H_2 + H + Ne + 4.24\ eV,$ (4b)
$\rightarrow CH(C) + H_2 + H + Ne + 3.49\ eV,$ (4c)
$\rightarrow CH(A) + 3H + Ne + 0.03\ eV.$ (4d)

$Ne(^3P_2) + C_2H_6$
$\rightarrow CH(A) + CH_4 + H + Ne + 5.23\ eV,$ (5a)
$\rightarrow CH(B) + CH_4 + H + Ne + 4.92\ eV,$ (5b)
$\rightarrow CH(C) + CH_4 + H + Ne + 4.17\ eV,$ (5c)
$\rightarrow CH(A) + CH_3 + H_2 + Ne + 5.20\ eV,$ (5d)
$\rightarrow CH(B) + CH_3 + H_2 + Ne + 4.90\ eV,$ (5e)
$\rightarrow CH(C) + CH_3 + H_2 + Ne + 4.14\ eV,$ (5f)
$\rightarrow CH(A) + CH + 2H_2 + Ne + 1.43\ eV,$ (5g)
$\rightarrow CH(B) + CH + 2H_2 + Ne + 1.12\ eV,$ (5h)
$\rightarrow CH(C) + CH + 2H_2 + Ne + 0.36\ eV,$ (5i)
$\rightarrow CH(A) + CH_3 + 2H + Ne + 0.68\ eV,$ (5j)
$\rightarrow CH(B) + CH_3 + 2H + Ne + 0.38\ eV,$ (5k)

→ CH(A) + CH_2 + H_2 + H + Ne + 0.45 eV, (5l)
→ CH(B) + CH_2 + H_2 + H + Ne + 0.14 eV. (5m)

Ne($^3P_2$) + C_2H_4
→ CH(A) + CH_3 + Ne + 6.62 eV, (6a)
→ CH(B) + CH_3 + Ne + 6.31 eV, (6b)
→ CH(C) + CH_3 + Ne + 5.56 eV, (6c)
→ CH(A) + CH + H_2 + Ne + 1.97 eV, (6d)
→ CH(B) + CH + H_2 + Ne + 1.66 eV, (6e)
→ CH(C) + CH + H_2 + Ne + 0.91 eV, (6f)
→ CH(A) + CH_2 + H + Ne + 1.86 eV, (6g)
→ CH(B) + CH_2 + H + Ne + 1.56 eV, (6h)
→ CH(C) + CH_2 + H + Ne + 0.80 eV. (6i)

Ne($^3P_2$) + C_3H_4
→ CH(A) + C_2H_3 + Ne + 6.45 eV, (7a)
→ CH(B) + C_2H_3 + Ne + 6.15 eV, (7b)
→ CH(C) + C_2H_3 + Ne + 5.39 eV, (7c)
→ CH(A) + C_2H_2 + H + Ne + 4.94 eV, (7d)
→ CH(B) + C_2H_2 + H + Ne + 4.64 eV, (7e)
→ CH(C) + C_2H_2 + H + Ne + 3.88 eV, (7f)
→ CH(A) + C_2H + H_2 + Ne + 4.61 eV, (7g)
→ CH(B) + C_2H + H_2 + Ne + 4.30 eV, (7h)
→ CH(C) + C_2H + H_2 + Ne + 3.55 eV, (7i)
→ CH(A) + C_2H + 2H + Ne + 2.06 eV, (7j)
→ CH(B) + C_2H + 2H + Ne + 1.75 eV, (7k)
→ CH(C) + C_2H + 2H + Ne + 1.00 eV, (7l)
→ CH(A) + CH_3 + H + Ne + 0.62 eV, (7m)
→ CH(B) + CH_3 + H + Ne + 0.31 eV. (7n)

For the reactions with higher-energy metastable Ne($^3P_0$) atoms, 0.10 eV higher excess energies are released in the above reactions. Based on our previous experiment on the Ne($^3P_{0,2}$)/Xe^+($^2P_{3/2}$) excitation-transfer reaction,[19] the [Ne($^3P_0$)]/[Ne($^3P_2$] ratio in the flow system is expected to be ≈0.13.

The emission rate constants for reactions (4)–(7) were determined by using a reference reaction method. The NO(A-X) emission from the Ne($^3P_{0,2}$)/NO reaction was used as a reference reaction.[11]

Ne($^3P_{0,2}$) + NO → NO($A^2\Sigma^+$) + Ne (8)
k_8 = 4.8 × 10^{-11} cm^3 $molecule^{-1}$ s^{-1}

Emission rate constants were estimated by comparing the integrated emission intensity of each CH* band system with that of NO(A–X) in prepared mixtures of M/NO. When there is no nonradiative decay and pumping from the observation region, the emission rate constants correspond to the formation ones.

Emission rate constants thus obtained are given in Table 1. For comparison, corresponding data for C_2H_2 obtained in our previous work[11] is given. The total emission rate constant of CH(A,B,C) from C_2H_2, 1.72 × 10^{-13} cm^3 $molecule^{-1}$ s^{-1}, is largest. The $k_{CH*}(M)/k_{CH*}(C_2H_2)$ ratio decreases in the order of C_3H_4, C_2H_4, CH_4, and C_2H_6 from 0.34 to 0.22, 0.048, and 0.023, respectively. In all cases, the CH(A) state is major CH* products, which occupies 64−92% of CH(A,B,C). Minor CH(B) and CH(C) states occupy 7.9−36 and 0.061−1.2% of CH(A,B,C), respectively.

The quenching rate constant of Ne($^3P_{0,2}$) by CH_4 has been measured to be 11 × 10^{-11} cm^3 $molecule^{-1}$ s^{-1}.[20] A comparison between this values and the emission rate constant of CH* obtained in this work suggests that the branching ratio of dissociative excitation leading to CH(A,B,C) is only 7.5 × 10^{-3} % in the Ne($^3P_{0,2}$)/CH_4 reaction. Based on this fact, dissociative excitation (4a)−(4d) is minor product channel, so that Penning ionization and dissociation into non-emitting neutral products are expected to be major product channels in the Ne($^3P_{0,2}$)/CH_4 reaction. Unfortunately, quenching rate constants of Ne($^3P_{0,2}$) by C_2H_6, C_2H_4, and C_3H_4 have not been measured. Therefore, information on total quenching rate constants and Penning ionization rate constants is required to determine branching ratios of CH(A,B,C) formation in the Ne($^3P_{0,2}$)/M (M = C_2H_6, C_2H_4, and C_3H_4) reactions.

Table 1. Emission rate constants (× 10^{-13} cm^3 $molecule^{-1}$ s^{-1}) of CH(A,B,C) produced from the reactions of Ne($^3P_{0,2}$) with aliphatic hydrocarbons.

	CH_4	C_2H_6	C_2H_4	C_2H_2	C_3H_4
	This work	This work	This work	Ref. 11	This work
CH(A)	0.070	0.025	0.35	1.5	0.53
CH(B)	0.012	0.014	0.030	0.22	0.052
CH(C)	3.3 E(-4)	4.5 E(-4)	2.3 (E-4)	4.6 (E-3)	6.8 (E-3)
sum	0.082	0.039	0.38	1.72	0.59

3.3 Rovibrational distributions of CH(A,B) in the Ne($^3P_{0,2}$)/M (M = CH_4, C_2H_6, C_2H_4, and C_3H_4) reactions

Rovibrational distributions of CH(A,B) in the Ne($^3P_{0,2}$)/M (M = C_2H_6, C_2H_4, and C_3H_4) reactions were determined by a computer simulation of CH(A–X, B–X) bands because rotational lines were not fully resolved. The simulation method used in this study was the same as that reported in our previous studies on CH_4[10] and C_2H_2.[11]

In Figs. 6–11 are shown the observed and

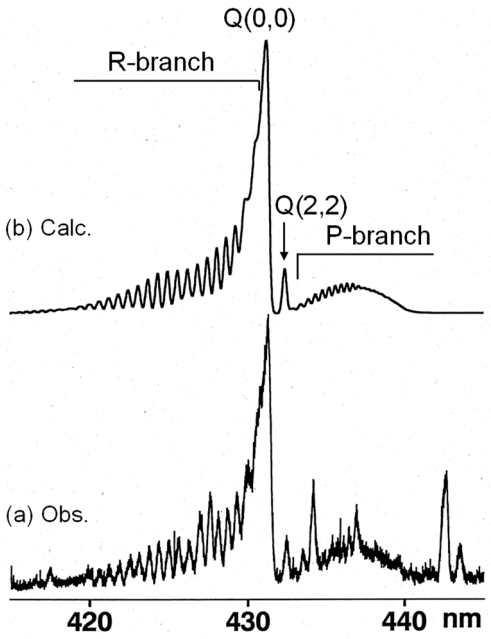

Fig. 6. (a) observed and (b) simulated emission spectra of CH($A^2\Delta$–$X^2\Pi_r$) band system in the Ne($^3P_{0,2}$)/C_2H_6 reaction.

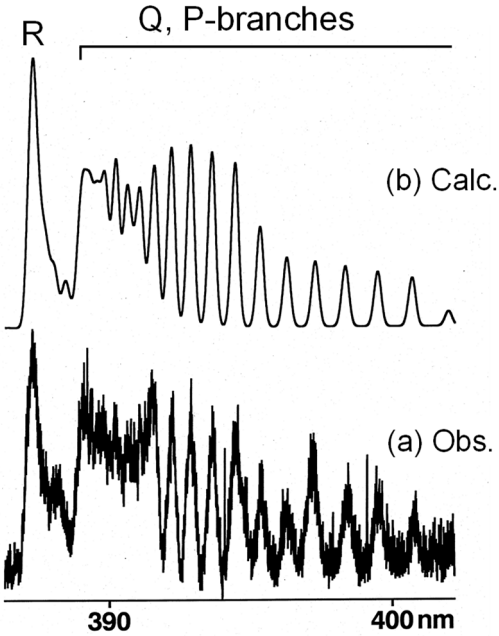

Fig. 7. (a) observed and (b) simulated emission spectra of (0,0) band of CH($B^2\Sigma^-$–$X^2\Pi_r$) band system in the Ne($^3P_{0,2}$)/C_2H_6 reaction.

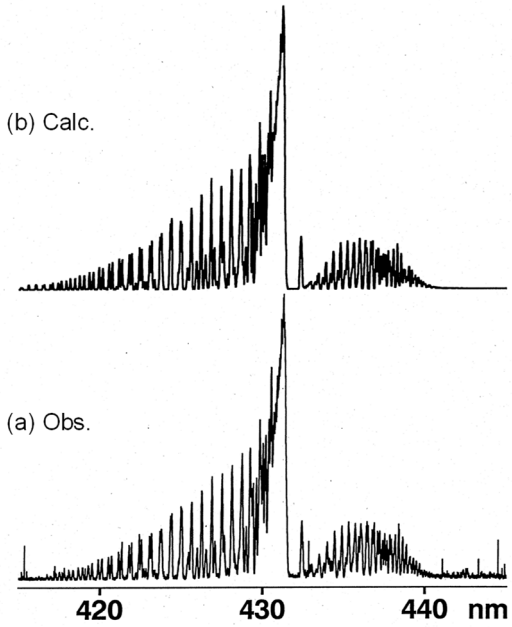

Fig. 8. (a) observed and (b) simulated emission spectra of CH($A^2\Delta$–$X^2\Pi_r$) band system in the Ne($^3P_{0,2}$)/C_2H_4 reaction.

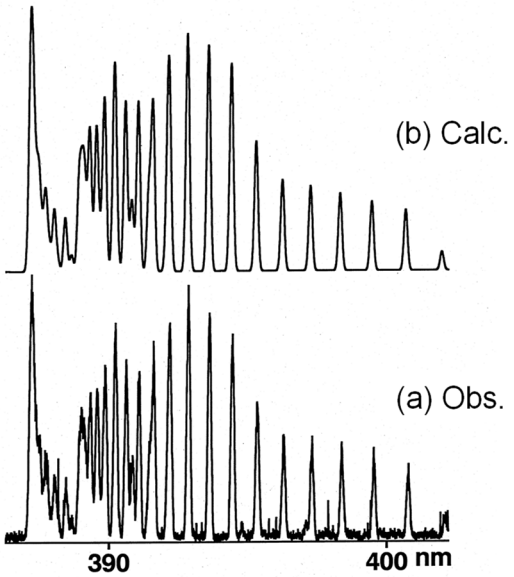

Fig. 9. (a) observed and (b) simulated emission spectra of (0,0) band of CH($B^2\Sigma^-$–$X^2\Pi_r$) band system in the Ne($^3P_{0,2}$)/C_2H_4 reaction.

best fit spectra of the CH(A–X, B–X) bands from C_2H_6, C_2H_4 and C_3H_4 calculated assuming single Boltzmann rotational distributions for each v' level. Vibrational and rotational temperatures thus obtained are given in Table 2 along with our previous data for CH_4[10] and C_2H_2.[11] From the observed rovibrational distributions of CH(A,B), we evaluated the average vibrational and rotational energies of each CH* state, denoted as $<E_v>$ and $<E_r>$, respectively. The $<E_v>$ and $<E_r>$ values obtained for CH(A,B) are summarized in Tables 3 along with our previous data for CH_4 and C_2H_2.[10,11] As discussed in our previous paper,[11] it is expected that the vibrational and rotational relaxation of CH(A,B) by collisions with the buffer Ne gas is insignificant within their radiative lifetimes of about 500 ns for CH(A)[21] and 345–357 ns for CH(B),[22] so that observed rovibrational distributions reflect nascent distributions.

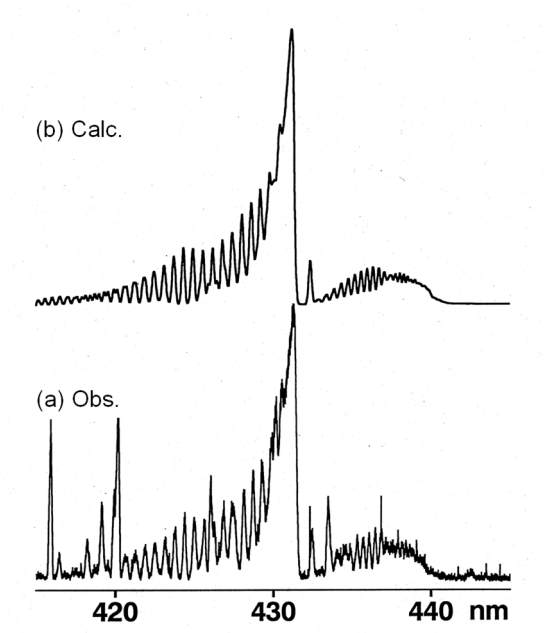

Fig. 10. (a) observed and (b) simulated emission spectra of CH($A^2\Delta$–$X^2\Pi_r$) band system in the Ne($^3P_{0,2}$)/C_3H_4 reaction.

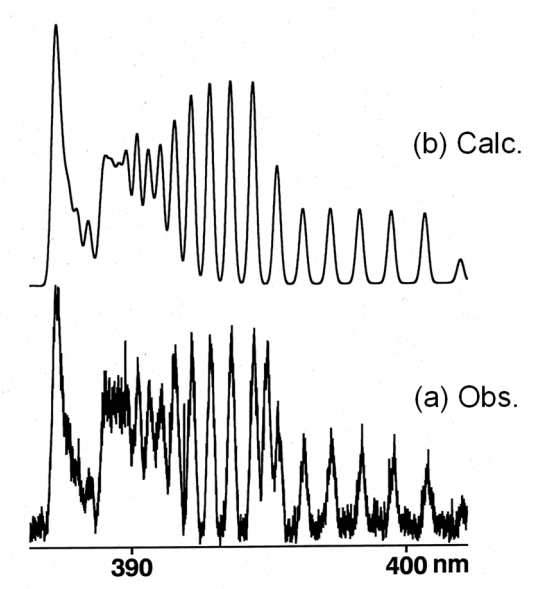

Fig. 11. (a) observed and (b) simulated emission spectra of (0,0) band of CH($B^2\Sigma^-$–$X^2\Pi_r$) band system in the Ne($^3P_{0,2}$)/C_3H_4 reaction.

The following tendencies are found for the observed rovibrational distributions of CH*.

(1) The vibrational population of CH(A:v'=0–2) decreases with increasing v'. The rotational temperature of CH(A) decreases from 3300–4600 K to 1700–2500 K with increasing v' from 0 to 2. The rotational temperature of CH(B: v'=0) is 2500–5500 K.

(2) The CH(A) states from CH_4 and C_2H_2 are more vibrationally excited than those from C_2H_6, C_2H_4 and C_3H_4. The rotational temperature of CH(A:v'=0) for CH_4, C_2H_2, and C_3H_4 (4200–4600 K) are higher than those for C_2H_6 and C_2H_4 (3300–3400 K). The CH(A:v'=0 and B:v'=0) states from C_3H_4 are more rotationally excited than those from the other aliphatic hydrocarbons.

(3) The $<E_v>$ values of CH(A) for CH_4 and C_2H_2 (0.13–0.15) are larger than those for C_2H_6, C_2H_4 and C_3H_4 (0.09–0.10). The $<E_r>$ values of CH(A) for CH_4, C_2H_2, and C_3H_4 (0.31–0.34) are larger than those for C_2H_6 and C_2H_4 (0.26–0.27). The $<E_r>$ value of CH(B) for C_3H_4 (0.47) is larger than those for CH_4, C_2H_2, and C_2H_4 (0.22–0.26).

(4) Tokeshi et al.[23] measured vibrational and rotational distributions of CH(A) from C_2H_6, C_2H_4, and C_2H_2 by electron impact at 17–100 eV range. The N_1/N_0 and N_2/N_0 values at 17 eV, which are close to the energies of Ne($^3P_{0,2}$), were 0.30 and 0.058 for C_2H_6, 0.29 and 0.044 for C_2H_4, and 0.44 and 0.078 for C_2H_2, respectively. These values are in reasonable agreement with those obtained from the Ne($^3P_{0,2}$) reactions (Table 2).

The rotational temperatures of CH(A:v'=0) and CH(A:v'=1) under electron impact at 17 eV were 4400 and 3200 K for C_2H_6, 5100 and 3400 K for C_2H_4, and 3200 and 2000 K for C_2H_2, respectively. Rotational temperatures obtained from the

Table 2. Rovibrational distributions of CH(A,B) produced from the Ne($^3P_{0,2}$)/aliphatic hydrocarbons reactions.

		CH_4 Ref. 10		C_2H_6 This work		C_2H_4 This work		C_2H_2 Ref. 11		C_3H_4 This work	
Emitting species		$N_{v'}$	T_r/ K	$N_{v'}$	T_r/ K	$N_{v'}$	T_r/ K	$N_{v'}$	T_r/ K	$N_{v'}$	T_r/ K
CH(A)	v'=0	100	4200	100	3400	100	3300	100	4200	100	4600
	v'=1	58	2800	27	2200	32	2200	45	3000	28	2200
	v'=2	9	2400	6	1750	4	1700	7	2500	4	1700
CH(B)	v'=0	100	3000	100	3000	100	2750	100	2500	100	5500

Table 3. Average vibrational and rotational energies (eV) deposited into CH (A, B) in the Ne($^3P_{0,2}$)/aliphatic hydrocarbons reactions.

	CH_4 Ref. 10		C_2H_6 This work		C_2H_4 This work		C_2H_2 Ref. 11		C_3H_4 This work	
Emitting species	$<E_v>$	$<E_r>$	$<E_v>$	$<E_r>$	$<E_v>$	$<E_r>$	$<E_v>$	$<E_r>$	$<E_v>$	$<E_r>$
CH(A)	0.15	0.31	0.10	0.27	0.10	0.26	0.13	0.32	0.09	0.34
CH(B)	0.0	0.26	0.0	0.26	0.0	0.24	0.0	0.22	0.0	0.47

Ne($^3P_{0,2}$) reactions are lower than those by electron impact excitation by 1000 K for C_2H_6 and by 1200–1800 K for C_2H_4, whereas they are higher than those by electron impact excitation by 1000 K for C_2H_2 (Table 2).

3.4 The formation mechanisms of CH* from simple aliphatic hydrocarbons

The formation mechanisms of CH* from aliphatic hydrocarbons are discussed from molecular structure and electronic structure of superexcited states of each hydrocarbon. As shown in energy-level diagrams (Figs. 2–5), energies of Ne($^3P_2$ = 16.60 eV, $^3P_0$ = 16.72 eV) are higher than those of the first IPs of CH_4, C_2H_6, C_2H_4, and C_3H_4 by 4.1–6.7 eV. Therefore, not only the ground ionic states but also some excited ionic states can be formed by Penning ionization between Ne($^3P_{0,2}$) and M.

$$Ne(^3P_{0,2}) + M \rightarrow M^+ \text{ and } M^{+*} + Ne + e^- \quad (9)$$
(M = CH_4, C_2H_6, C_2H_4, and C_3H_4)
Penning ionization

In addition, the formation of superexcited M** states below 16.72 eV is also possible, from which autoionization and dissociation occur competitively.

$$Ne(^3P_{0,2}) + M \rightarrow M^{**} + Ne \quad (10a)$$
(M = CH_4, C_2H_6, C_2H_4, and C_3H_4)
$$M^{**} \rightarrow M^+ \text{ and } M^{+*} + e^- \text{ (autoionization)} \quad (10b)$$
$$M^{**} \rightarrow m_1 + m_2 \text{ (dissociation)} \quad (10c)$$

where m_1 and m_2 are neutral fragments.

There are two possible energy-transfer mechanisms in process (10a). One is near-resonant energy transfer without significant momentum transfer. The other is non-resonant energy transfer with a significant momentum transfer

$$Ne(^3P_{0,2}) + M \rightarrow M^{**} + Ne + \Delta T \quad (11a)$$
$$M^{**} \rightarrow CH(A,B,C) + \text{neutral fragments} \quad (11b)$$

where ΔT represents a translational energy released after energy transfer. If entrance Ne($^3P_{0,2}$) + M potentials are strongly attractive, such non-resonant energy transfer can occur through accidental avoided crossing between attractive entrance surfaces and low energy M** + Ne exit potentials. Actually, such non-resonant energy transfer has been observed in the reactions for open shell atoms and molecule: e.g., Ar($^3P_{0,2}$) + O and Cl and Ar($^3P_2$) + C_2H_5 and Kr($^3P_2$) + C_2H_5.[24,25] For the cases of M (M = CH_4, C_2H_6, C_2H_4, and C_3H_4), ground states are closed shell singlet states. Therefore, rather flat entrance Ne($^3P_{0,2}$) + M potentials are

expected. It is therefore reasonable to assume that energy-transfer from Ne($^3P_{0,2}$) to M take place via near-resonant excitation processes without significant momentum transfer.

Based on our optical spectroscopic studies on the dissociative excitation of simple polyatomic molecules by rare gas metastable He(2^3S) and Rg($^3P_{0,2}$) atoms,[26-30] spin-conservation rule generally holds during the reaction. Therefore, triplet superexcited M** states below 16.72 eV are expected to be formed after near-resonant energy transfer, because the ground states of M are singlet. Although superexcited states of CH_4, C_2H_6, and C_2H_4 have been extensively studied by using vacuum ultraviolet photons and fast electron-impact excitation,[23,31-40] they are spin-allowed singlet states. It is highly likely that similar triplet superexcited states exist just below corresponding singlet states, although little information has been obtained on the triplet superexcited states of aliphatic hydrocarbons in the 13−17 eV range.

3.4.1 CH_4

The ground state methane in T_d symmetry has the electronic configuration,[36]

$$^1A_1: (1a_1)^2(2a_1)^2(1t_2)^6. \quad (12)$$

Kato et al.[37] studied superexcited states of CH_4 around 14.5 eV built on the $(1t_2)^{-1}$ ion core and those around 22 eV built on the $(2a_1)^{-1}$ ion core using synchrotron orbital radiation (SOR). Although these superexcited states are optically allowed singlet states, similar triplet superexcited states are expected to exist below the corresponding singlet states. They concluded that CH(A) and CH(B) are produced from single-hole one-electron states built on the $(1t_2)^{-1}$ ion core ion in the 13–16 eV region under vacuum ultraviolet (VUV) photoexciation. It is reasonable to assume that CH(A) and CH(B) are also produced from similar single-hole one-electron states built on the $(1t_2)^{-1}$ ion core in the Ne($^3P_{0,2}$)/CH_4 reaction. However, these superexcited states in the 13–16.7 eV are unknown triplet states, which are not observed under VUV photoexciation. Since the $1t_2$ molecular orbital has π_{CH_3}(pseudo) character,[17] C–H bond-length and H–C–H angles will change when an electron is ejected from this orbital. These geometric changes led to vibrational and rotational excited CH(A,B) fragments from dissociation of CH_4**.

3.4.2 C_2H_6

The electronic configuration of the ethane molecule in the ground state is

$$^1A_{1g}: (1a_{1g})^2(1a_{2u})^2(2a_{1g})^2(2a_{2u})^2 \times (1e_u)^4(3a_{1g})^2(1e_g)^4 \quad (13)$$

for the staggered D_{3d} symmetry.[23,32] The vertical ionization potentials of these orbitals were determined by photoelectron spectroscopy as 11.99 (12.70) eV for the $(1e_g)^{-1}$ state, 13.5 eV for the $(3a_{1g})^{-1}$ state, and 15.15 (15.9) eV for the $(1e_u)^{-1}$ state; Jahn-Teller components are given in parentheses.[17] On the basis of detailed VUV photoexcitation studies on C_2H_6,[36] neutral superexcited states of C_2H_6** exist in the 11–16 eV region which cover all Rydberg states converging to the above ionic states. Unknown triplet Rydberg states converging to the $(1e_u)^{-1}$ state will be most important precursor states leading to CH(A,B) based on energy-resonant rule. Molecular structures of Rydberg states will be similar to those of related ionic states. Since the $1e_u$ molecular orbital has $\pi_{CH_3}^+$(pseudo) character, C–H bond length and H–C–H angle will change after an electron is ejected from this orbital. Geometrical changes after excitation into $(1e_u)^{-1}$ ion core Rydberg states led to vibrational and rotational excited CH(A,B) fragments from C_2H_6**.

3.4.3 C_2H_4

The electronic configuration of the ethylene molecule in the ground state is

$$^1\Sigma_g^+: (1a_g)^2(1b_{1u})^2(2a_g)^2(2b_{1u})^2(1b_{2u})^2 \times (3a_g)^2(1b_{3g})^2(1b_{3u})^2 \quad (14)$$

for the D_{2h} symmetry.[40] The vertical ionization potentials of these orbitals below 17 eV were determined by photoelectron spectroscopy as 10.51 eV for the $(1b_{3u})^{-1}$ state, 12.85 eV for the $(1b_{3g})^{-1}$ state, 14.66 eV for the $(3a_g)^{-1}$ state, and 15.87 eV for the $(1b_{2u})^{-1}$ state.[17]

The formation of CH(A,B) from VUV photodissociation of C_2H_4 in the 11.7–21.4 eV range has been studied by O'Reilly et al.[38] Two dissociation processes have been observed for the formation of CH(A,B).

	Thermodynamic threshold	
$C_2H_4 \rightarrow CH(A) + CH_3$	10.0 eV	(15a)
$\rightarrow CH(B) + CH_3$	10.3 eV	(15b)
$\rightarrow CH(A) + CH + H_2$	14.6 eV	(16a)
$\rightarrow CH(B) + CH + H_2$	14.9 eV	(16b)

The observed threshold energies for (15a) and (15b) were 10.4±0.5 eV and <12 eV, whereas those for (16a) and (16b) were 14.6±0.8 eV and 14.6±0.8 eV, respectively. Processes (16a) and (16b) are more near resonant than processes (15a) and (15b) in the $Ne(^3P_{0,2})/C_2H_4$ reactions. Therefore, they will be major formation processes of CH(A,B) in the $Ne(^3P_{0,2})/C_2H_4$ reaction, if the $Ne(^3P_{0,2})/C_2H_4$ reaction proceeds through similar processes as observed VUV photodissociation. Unknown triplet Rydberg states in the 14.6–16.7 eV converging to the $(3a_g)^{-1}$ and $(1b_{2u})^{-1}$ ionic states would be intermediates for the formation of CH(A,B). Since the $(3a_g)^{-1}$ and $(1b_{2u})^{-1}$ molecular orbital have σ_{CC} and $\pi_{CH_2}^{+}$(pseudo) characters, C=C and C−H bond lengths and H−C−H angels change, when an electron is ejected from $3a_g$ or $1b_{2u}$ orbital. Vibrational and rotational excitation of CH(A,B) fragments are expected from C_2H_4** Rydberg states because of geometrical changes in the C_2H_4** states after excitation from the ground C_2H_4 state.

3.4.4 C_3H_4

The electronic configuration of the allene molecule in the ground state is

$$^1A_1 : (la_1)^2(lb_2)^2(2a_1)^2(3a_1)^2(2b_2)^2 \times (4a_1)^2(3b_2)^2(le)^4(2e)^4 \quad (17)$$

for D_{2d} symmetry.[35] The vertical ionization potentials of these orbitals were determined by photoelectron spectroscopy as 10.06 and 10.60 eV for the $(2e)^{-1}$ state, 14.70 eV for the $(1e)^{-1}$ state, 15.47 eV for the $(3b_2)^{-1}$ state, and 17.47 eV for the $(4a_1)^{-1}$ state.[17]

The valence-shell photoabsorption, photodissociation and photoionization cross-sections of allene have been measured from the ionization threshold to 35 eV using SOR.[35] Although no information on the CH(A,B) from C_3H_4 has been obtained, small cross sections corresponding to dissociation into neutral products are observed in the 14–17 eV region. Dissociation cross sections are much smaller than ionization cross sections, indicating that neutral dissociation processes are minor exit channels in this energy region under VUV photoexciation. Dissociation including dissociative excitation may also be minor exit channel in the $Ne(^3P_{0,2})/C_3H_4$ reaction because the emission rate constant of CH(A,B,C) from C_3H_4 obtained here was very small.

Based on energy-resonant and spin-conservation rules, CH(A,B) will be formed via superexcited states in the 14.0–16.7 eV region. Possible candidates are triplet Rydberg states converging to the $(1e)^{-1}$, $(3b_2)^{-1}$, and $(4a_1)^{-1}$ states having π_{CH_2}, σ_{CC}, and C_{2s} characters, respectively. It should be noted that the CH(A: v' =0 and B: v' =0) states are more rotationally excited than the other hydrocarbons. High rotational excitation may arise from rotationally excitation of precursor superexcited C_3H_4** states and/or vibrational excitation of H−C−H bending modes of C_3H_4**.

4. Summary and Conclusion

Dissociative excitation of CH_4, C_2H_6, C_2H_4, and C_3H_4 by collisions with metastable $Ne(^3P_{0,2})$ atoms has been studied by observing CH(A–X,B–X,C–X) emissions in the Ne FA. The effect of SF_6 addition into the Ne afterglow indicated that secondary electron-ion recombination reactions do not participate in the formation of CH(A,B.C) and they are formed through the primary $Ne(^3P_{0,2})$/M (M = CH_4, C_2H_6, C_2H_4, and C_3H_4) reactions. The emission rate constants of CH(A,B,C) were determined by using a reference reaction method. A comparison between the observed emission rate constant and reported total quenching rate constant in the $Ne(^3P_{0,2})/CH_4$ reaction indicated that the branching ratio of dissociative excitation leading to CH(A,B,C) is only 7.5×10^{-3} %. Major exit channels in the $Ne(^3P_{0,2})/CH_4$ reaction was expected to be Penning ionization and dissociation into non-emitting neutral products. The nascent vibrational and rotational distributions of CH(A: v' =0–2,B: v' =0) were determined. Vibrational and rotational excitation of CH(A,B) originates from geometrical changes in CC, CH, and HCH bonds after excitation into M** superexcited states. A high rotational excitation of CH(A,B) from C_3H_4 suggested that precursor superexcited C_3H_4** is rotationally excited and/or vibrational excitation of H−C−H bending modes of C_3H_4**.

Acknowledgments

Authors thank Prof. Takeshi Odagiri (Sophia Univ.) for sending a copy of Ref. 37. This work was supported by the Mitsubishi foundation (1996) and JSPS KAKENHI Grant number 09440201 (1997-2000).

References

1) N. Mutsukura and K. Miyatani, *Diamond Relat. Mater.*, 4, 342 (1995).

2) P. Yang , S. C. H . Kwok, R. K. Y. Fu , Y. X. Leng, J. Wang, G. J. Wan, N. Huang, Y. Leng, and P. K. Chu, *Surf. Coat. Tech.*, 177/178, 747 (2004).
3) S. Avtaeva and V. Gorokhovsky, *Plasma Chem. Plasma Process.*, 41, 815 (2021).
4) R. S. F. Chang, D. W. Setser, and G. W. Taylor, *Chem. Phys.*, 25, 201 (1978).
5) D. H. Winicur, J. L. Hardwick, and S. N. Murphy, *Comb. Flame*, 53, 93 (1983).
6) D. H. Winicur and J. L. Hardwick, *Chem. Phys.*, 94, 157 (1985).
7) L. G. Piper, 1. E. Velazco, and D. W. Setser, *J. Chem. Phys.*, 59, 3323 (1973).
8) T. Ueno, A. Yokoyama, S. Takao, and Y. Hatano, *Chem. Phys.*, 45, 261 (1980).
9) M. Tsuji, K. Kobarai, H. Obase, H. Kouno, and Y. Nishimura, *J. Chem. Phys.*, 94, 277 (1991).
10) M. Tsuji, T. Komatsu, M. Tanaka, M. Nakamura, Y. Nishimura, and H. Obase, *Chem. Lett.*, 26, 359 (1997).
11) M. Tsuji, T. Komatsu, K. Uto, J.-I. Hayashi, and T. Tsuji, *Eng. Sci. Rep., Kyushu Univ.*, 43, 8 (2021).
12) M. Tsuji, T. Komatsu, K. Uto, J.-I. Hayashi, and T. Tsuji, *Eng. Sci. Rep., Kyushu Univ.*, 43, 23 (2021).
13) H. Obase, M. Tsuji, and Y. Nishimura, *Chem. Phys.*, 74, 89 (1983).
14) H. L. Snyder, B. T. Smith, T. P. Parr, and R. M. Martin, *Chem. Phys.*, 65, 397 (1982).
15) *NIST Chemistry WebBook*, NIST Standard Reference Database, Number 69 (2018): http://webbook.nist.gov/chemistry.
16) K. P. Huber and G. Herzberg, "*Molecular Spectra and Molecular Structure, IV. Constants of Diatomic Molecules*", Van Nostrand Reinhold, New York (1979).
17) K. Kimura, S. Katsumata, Y. Achiba, T. Yamazaki, and S. Iwata: "*Handbook of He Photoelectron Spectra of Fundamental Organic Molecules. Ionization Energies, Ab Initio Assignments, and Valence Electronic Structure for 200 Molecules*", Japan Scientific Societies Press, Tokyo und Halstead Press, New York (1981).
18) F. C. Fehsenfeld, *J. Chem. Phys.*, 53, 2000 (1970).
19) M. Tsuji, N. Kaneko, and Y. Nishimura, *J. Chem. Phys.*, 101, 7451 (1994).
20) P. Tosi, D. Bassi, B. Brunetti, and F. Vecchiocattivi, *Int. J. Mass Spectrom. Ion Process.*, 149/150, 345 (1995).
21) J. Carozza and R. Anderson, *J. Opt. Soc. Amer.*, 118 (1977).
22) M. Ortiz and J. Campos, *Physica B+C*, 114, 135 (1982).
23) M. Tokeshi, K. Nakashima, and T. Ogawa, *Chem. Phys.*, 203, 257 (1996).
24) D. L. King, L. G. Piper, and D. W. Setser, *J. Chern. Soc. Faraday Trans. II*, 73, 177 (1977).
25) M. Tsuji, H. Kouno, H. Ujita, and Y. Nishimura, *J. Chem. Phys.*, 96, 6746 (1992).
26) M. Tsuji, K. Kobarai, S. Yamaguchi, H. Obase, K. Yamaguchi, and Y. Nishimura, *Chem. Phys. Lett.*, 155, 481 (1989).
27) M. Tsuji, K. Kobarai, S. Yamaguchi, and Y. Nishimura, *Chem. Phys. Lett.*, 158, 470 (1989).
28) M. Tsuji, K. Kobarai, and Y. Nishimura, *J. Chem. Phys.*, 93, 3133 (1990).
29) M. Tsuji, K. Kobarai, S. Yamaguchi, H. Obase, and Y. Nishimura, *Chem. Phys. Lett.*, 166, 485 (1990).
30) M. Tsuji, K. Kobarai, H. Kouno, H. Obase, and Y. Nishimura, *Jpn. J. Appl. Phys.*, 30, 862 (1991).
31) Y. Hatano, *Bull. Chem. Soc. Jpn.*, 41, 1126 (1968).
32) J. Berkowitz, "*Photoabsorption, Photoionization and Photoelectron Spectroscopy*", Academic Press, New York. (1979).
33) K. Kameta, S. Machida, M. Kitajima, M. Ukai, N. Kouchi, Y. Hatano, and K. Ito, *J. Electron Spectrosc. Relat. Phenom.,* 79, 391 (1996).
34) D. M. P. Holland, D. A. Shaw, M. A. Hayes, L. G. Shpinkova, E. E. Rennie, L. Karlsson, P. Baltzer, and B. Wannberg, *Chem. Phys.*, 219, 91 (1997).
35) D. M. P. Holland and D. A. Shaw, *Chem. Phys.*, 243, 333 (1999).
36) K. Kameta, N. Kouchi, M. Ukai, and Y. Hatano, *J. Electron Spectrosc. Relat. Phenom.,* 123, 225 (2002).
37) M. Kato, K. Kameta, T. Odagiri, N. Kouchi, and Y. Hatano, *J. Phys. B: At. Mol. Opt. Phys.*, 35, 4383 (2002).
38) J. O'Reilly, S. Douin, S. Boye, N. Shafizadeh, and D. Gauyacq, *J. Chem. Phys.*, 119, 820 (2003). C2H4
39) K. Alnama, S. Boyé, S. Douin, F. Innocenti, J. O'Reilly, A.-L. Roche, N. Shafizadeh, L. Zuin, and D. Gauyacq, *Phys. Chem. Chem. Phys.*, 6, 2093 (2004).
40) T. Ibuki, G. Cooper, and C. E. Brion, *Chem. Phys.*, 129, 295 (1989).